ACS Catalysis

pubs.acs.org/acscatalysis

Research Article

Breaking the Selectivity-Conversion Limit of Partial Methane Oxidation with Tandem Heterogeneous Catalysts

Kimberly T. Dinh, Mark M. Sullivan, Pedro Serna, Randall J. Meyer, and Yuriy Román-Leshkov*

Cite This: *ACS Catal.* 2021, 11, 9262–9270

Read Online

ACCESS | Metrics & More | Article Recommendations | Supporting Information

ABSTRACT: The inherently unfavorable thermodynamics for the direct partial oxidation of CH_4 with O_2 limits the system to high selectivities only at low conversions. We demonstrate a tandem strategy capable of circumventing this selectivity-conversion limit by performing sequential oxidation of CH_4 to CH_3OH over a selective Cu-exchanged zeolite followed by C-alkylation of CH_3OH with benzene over an acidic zeolite. Using a small-pore zeolite (SSZ-13, CHA topology) to host the Cu species is essential to achieve increased yields by maximizing CH_4-to-CH_3OH selectivities while also protecting the final alkylate product from overoxidation via size-exclusion. Cofeeding CH_4, oxygen, water, and benzene over a mixture of Cu-SSZ-13 and H-ZSM-5 resulted in 77% toluene selectivity at 663 K and 1 bar compared to only 2% CH_3OH selectivity in the absence of benzene under identical conditions at isoconversion. A record productivity of 1.7 μmol min^{-1} g_{cat}^{-1} was achieved at 11 bar and 603 K (80% toluene selectivity at 0.37% CH_4 conversion), which represents a 30-fold improvement over current continuous processes over Cu-based zeolites. Our findings demonstrate the importance of protecting the methanol product to achieve high selectivities and help close the gap to realize more efficient small-scale CH_4 conversion processes.

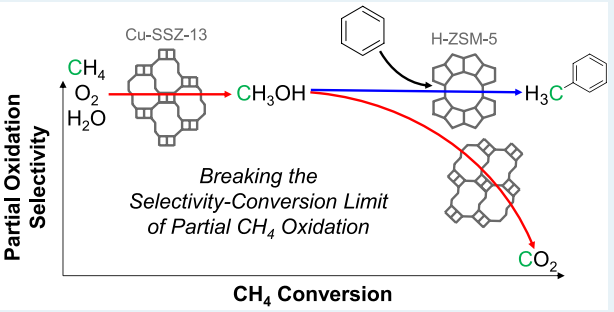

KEYWORDS: *methane, oxidation, Cu-exchanged zeolites, scavenging, product protection, alkylation, size-exclusion, tandem chemistry*

INTRODUCTION

The selective partial oxidation of CH_4 is an unresolved grand challenge in catalysis. The relative ease by which partially oxidized CH_4-derived products can undergo overoxidation in comparison to CH_4 implies that high selectivities can only be obtained at low single-pass conversions.[1−3] Latimer et al. quantified this selectivity-conversion limit using first principles, showing that the barrier for CH_3OH activation is generally lower than the barrier for CH_4 activation, which limits CH_3OH selectivities to >80% for CH_4 conversions <0.1% at ∼500 K.[4] Biological systems such as methane monooxygenases (MMOs) circumvent this selectivity-conversion limit by using a gating mechanism that flawlessly separates CH_3OH from the active site to arrest continued oxidation.[5] Although extensive research has been devoted to developing synthetic active sites that mimic those in MMOs, recreating the enzyme's gating mechanism in artificial systems has remained elusive.

Several strategies have been proposed to circumvent the CH_4 selectivity-conversion limit in continuous systems. One strategy is the direct formation of oxidation-resistant CH_3OH-derived products. The Pt-based Periana catalyst exemplifies this strategy, achieving 80% selectivity at 90% CH_4 conversion by converting CH_4 to methyl bisulfate using concentrated H_2SO_4. However, this process requires conditions that are difficult to implement industrially.[6] Similarly, CH_3OH selectivities >60% at ∼5 to 10% CH_4 conversion were reported for homogeneous systems in the presence of gas phase sensitizers aimed at initiating free radical reactions, but the process was limited by high pressures and operation within hazardous flammability limits.[7] Nørskov and co-workers suggested the introduction of a CH_3OH collector to limit gas phase overoxidation,[4] while van Bokhoven and co-workers emphasized the use of a multicomponent catalyst to protect CH_3OH.[8] Similarly, Dinh et al.[9] discussed an alternative solution involving chemical scavenging of CH_3OH, wherein a second species reacts with the alcohol product prior to continued oxidation. Chemical scavenging is particularly attractive as it may avoid the necessity of reactant and temperature cycling to desorb CH_3OH and reactivate the catalyst. To successfully implement a chemical scavenging system for partially oxidizing CH_4, the system must meet multiple requirements, namely: (1) CH_4 activation is uninhibited by the scavenger molecule, (2) the scavenger

Received: May 14, 2021
Revised: June 18, 2021

https://doi.org/10.1021/acscatal.1c02187
ACS Catal. 2021, 11, 9262–9270

molecule and product are more resistant than CH_3OH to undesirable oxidation to CO_2, and (3) the flux of reagents is optimized to promote the reaction of CH_3OH with the scavenger molecule over undesirable CH_3OH overoxidation events. Notably, the rate of the scavenging reaction must not be rate-limiting and the scavenging reaction events must be maximized relative to CH_3OH overoxidation events, for instance, by minimizing the diffusion distance between CH_3OH formation and scavenging sites.

Here, we demonstrate a continuous chemical scavenging strategy involving tandem partial oxidation and alkylation reactions over copper-exchanged and proton-exchanged zeolites.

This system maintains high product selectivity at increased CH_4 conversion values compared to standard continuous partial oxidation processes by effectively scavenging CH_3OH in the form of toluene. Although Cu-SSZ-13 (CHA topology) produces CH_3OH continuously with >75% selectivity using O_2,[10,11] this selectivity decreases quickly with CH_4 conversion beyond 0.01%.[4,11] However, intercepting the partially oxidized intermediates to form methyl-substituted aromatics via acid-catalyzed alkylation of benzene[12−14] creates products that are too large to access the sites in the zeolite interior responsible for overoxidation reactions. Cu-SSZ-13 is particularly well-suited to operate effectively in this system because neither benzene nor the alkylation products can access the Cu sites within the SSZ-13 cages (CHA pore window diameter of 3.72 Å[15] vs kinetic diameter of benzene of 5.85 Å[16]) to undergo combustion or inhibit selective CH_4 activation. Under optimized conditions, cofeeding benzene with CH_4, H_2O, and O_2 at mild conditions over a mixture of Cu-SSZ-13 and H-ZSM-5 (MFI topology) achieved a 30× improvement of product yields over state-of-the-art continuous oxidation processes with Cu-zeolites. This strategy allows accessing partial oxidation selectivities beyond the selectivity-conversion limit of traditional CH_4 partial oxidation systems and provides a pathway toward achieving more industrially relevant small-scale CH_4 conversion processes.

EXPERIMENTAL METHODS

Synthesis of Cu-SSZ-13. Cu-SSZ-13 was synthesized in a one-pot method as previously described by Dinh et al.[11] and is a modification of the works of Di Iorio et al.[17] and Martínez-Franco et al.[18] One-pot methods were reported for the synthesis for Cu-SSZ-13 via the use of tetraethylenepentamine (TEPA).[19]

Copper sulfate pentahydrate (98% trace metals basis, Sigma-Aldrich) was first dissolved in water followed by the addition of TEPA (technical grade, Sigma-Aldrich) and stirred for 1 h before the addition of *N,N,N*-trimethyl-1-adamantanamine hydroxide solution (TMAdaOH, 25 wt % in H_2O, Sachem). Following, aluminum hydroxide (80.3 wt % $Al(OH)_3$, SPI Pharma 0250) was dissolved in the solution before fumed silica (Sigma-Aldrich, 99.8%) was added. The final composition of the mixture was 1 SiO_2:0.07 $Al(OH)_3$:0.4 TMAdaOH:44 H_2O:0.01 $CuSO_4$:0.011 TEPA. The solution was stirred at room temperature for 2 h, transferred to four 23 mL Teflon-lined stainless-steel autoclaves (No. 4749, Parr Instruments) and subjected to hydrothermal treatment at 433 K for 5 days in an oven under autogenous pressure and rotation (60 rpm). After hydrothermal treatment, the product was separated from the mother liquor by centrifugation, washed several times with distilled H_2O until pH < 9, and dried overnight at 393 K. The zeolite was calcined under dry air (Dry Size 300, Airgas) with the following temperature profile: heat 1 K min^{-1} to 423 K and hold for 1 h at 423 K, heat 1 K min^{-1} to 623 K and hold for 1 h at 623 K, and lastly heat 1 K min^{-1} to 853 K and hold for 10 h.

Synthesis of H-ZSM-5. To 41.343 g water, 6.663 g tetrapropylammonium hydroxide (TPAOH, 40 wt % in water, SACHEM) was added and stirred for 15 min. Following, 0.135 g aluminum hydroxide (SPI Pharma 250) was added followed by 2.25 g sodium hydroxide solution in water (NaOH, Sigma-Aldrich, 23.0 wt % in water). The mixture was stirred for at least 10 mins; 2.604 g fumed silica (Cab-o-Sil M5) was then slowly added and shaken vigorously. The final gel composition was 1 SiO_2:0.04 $Al(OH)_3$:0.3 TPAOH:0.3 NaOH. The gel was allowed to homogenize and age with stirring for 16 h before being transferred to 23 mL Teflon-lined stainless-steel autoclaves (No. 4749, Parr Instruments) and subjected to hydrothermal treatment under static conditions at 453 K for 2 days in an oven under autogenous pressure. After hydrothermal treatment, the product was separated from the mother liquor by centrifugation, washed several times with distilled H_2O until pH < 9, and dried overnight at 393 K. The zeolite was calcined under dry air (Dry Air Size 300, Airgas) with the following temperature profile: heat 1 K min^{-1} to 423 K and hold for 1 h at 423 K, heat 1 K min^{-1} to 623 K and hold for 1 h at 623 K, and lastly heat 1 K min^{-1} to 853 K and hold for 10 h.

Following calcination, to remove Na, 1 g of zeolite was stirred in 60 mL of a 1.0 M solution of ammonium nitrate (≥99%, Sigma-Aldrich) for 16 h at room temperature. The suspension was filtered at room temperature, rinsed with 300 mL of deionized H_2O, and the recovered zeolite was immediately subjected to the same ion exchange twice more under the same conditions. Following, the zeolite was dried overnight at 393 K in stagnant air and calcined following the same temperature profile described above.

Catalytic Partial Oxidation Reactions. All reactions were conducted in a continuous, tubular flow reactor (304 stainless steel tube, O.D. 0.25 in., I.D. 0.18 in.). The reactor tube was mounted inside a single-zone furnace (850 W/115 V, Applied Test Systems Series 3210). Temperature was controlled using a thermocouple (Omega, model TJ36-CASS-116U) mounted slightly downstream of the catalyst bed connected to a temperature controller (Digi-Sense model 68900-10). The mixture of a copper-exchanged zeolite and a proton-form zeolite were mixed in a ratio of 1:3 by weight, ground with a mortar and pestle, and then vortexed to ensure a homogeneous catalyst mixture. This zeolite mixture (0.35 g, pelletized and sieved into 250−420 μm particles) was packed between quartz wool plugs and rested on a thermocouple in the middle of the furnace heating zone. Control reactions were performed with the same absolute loadings of the individual catalysts, and catalyst beds were pelletized to the same size distribution. Void volume above and below the catalyst bed was filled with borosilicate glass beads to reduce homogeneous combustion. Blank reactors were loaded in the same manner in the absence of the catalyst. For testing with increased catalyst loading, a 304 stainless steel, O.D. 0.5 in., I.D. 0.40 in. reactor was used.

The flow of gases, including He (ultra high purity, Airgas), 1% O_2 in He (ultra high purity, Airgas), and CH_4 (research grade, Airgas) were controlled with independent mass flow controllers (Brooks Instruments LLC). H_2O (typically 3.2 kPa, the saturation vapor pressure at 298 K) was introduced into the gas stream via a stainless-steel saturator and benzene was introduced using a syringe pump (Harvard Apparatus) with a

https://doi.org/10.1021/acscatal.1c02187
ACS Catal. 2021, 11, 9262−9270

heated liquid injection port. System pressure was controlled with a back pressure regulator (Equilibar U3L Series) between the reactor and the gas chromatograph. Stainless steel gas transfer lines were heated with resistive heating tape from the point of liquid injection until the gas chromatographic analysis unit. Typical reaction pretreatment involved calcining the catalyst at 823 K for 8 h under 50 mL min^{-1} dry air.

CH_3OH, dimethyl ether (DME), CO, CO_2, benzene, toluene, and xylene partial pressures evolved during catalytic tandem oxidation and alkylation reactions were quantified using a gas chromatograph (Agilent Technologies, 7890B). The gas chromatograph was equipped with a methanizer, flame ionization detector, and thermal conductivity detector. Three columns were used for product separation: two HP-PLOT Q PT (30 m × 0.53 mm × 40 μm, Agilent #19095P-QO4PT) and HP-PLOT Molsieve (30 m × 0.53 mm × 50 μm, Agilent #19095P-MS0E).

All reported values for selectivity and rates of product formation were averaged over three data points upon reaching a steady-state.

Product Quantification. Calibration curves for CO_2, CH_3OH, CO, and DME were constructed by flowing known mixtures of 1% CO_2/He, 0.5% CH_3OH/He, 90 ppm CO/N_2, 10% DME/He and He, respectively, to a gas chromatograph. Calibration curves for benzene and toluene were constructed by injecting known liquid flow rates into a flowing gas stream with a known flow rate. A response factor for xylene was inferred from that of toluene by carbon weighting. The error of the observed rates is less than 2% based on estimation from the observed rates over separate batches of Cu-SSZ-13 and H-ZSM-5 under two different conditions.

The large partial pressure of CH_4 in the gas stream during catalytic CH_4 oxidation reactions prevented the accurate quantification of CH_4 consumption. As such, CH_4 conversion was assumed to be equal to the total molar flow rate of carbon of all observed products divided by the initial molar flow rate of CH_4:

$$X_{CH_4} = \frac{\sum_{i=1}^{N} C_i F_i}{F_{CH_{4,0}}}$$

where X_{CH_4} is the conversion of CH_4, F_i is the molar flow rate of product i, C_i is the number of carbon atoms incorporated from CH_4 into product i, $\Sigma C_i F_i$ is the total molar flow rate of carbon of all products, and $F_{CH_{4,0}}$ is the initial molar flow rate of CH_4.

Product selectivity for catalytic CH_4 oxidation and tandem oxidation and alkylation was defined as:

$$S_i = \frac{C_i F_i}{\sum_{i=1}^{N} C_i F_i}$$

where S_i is the selectivity of product i on a C-atom basis, C_i is the number of carbon atoms incorporated from CH_4 into product i, F_i is the molar flow rate of product i, and $\Sigma C_i F_i$ is the total molar flow rate of carbon of all products.

Product yield for catalytic CH_4 oxidation and tandem oxidation and alkylation was defined as:

$$Y_i = \frac{C_i F_i}{N_{Cu} \text{or } g_{cat}}$$

where Y_i is the selectivity of product i on a C-atom basis, N_{Cu} is the number of moles of Cu within the zeolite determined by inductively coupled plasma (ICP), and g_{cat} is the catalyst loading.

RESULTS AND DISCUSSION

The successful implementation of the chemical scavenging strategy using Cu-SSZ-13 and H-ZSM-5 zeolites (Scheme 1) hinges on three critical requirements. First, the active sites of Cu-SSZ-13 must perform the partial oxidation of CH_4 selectively, desorbing the CH_3OH before it undergoes deleterious consecutive reactions. Second, the alkylation catalyst should not contain trace metal species capable of performing oxidation chemistry. Third, the flux of reagents should be optimized to promote the reaction of CH_3OH with benzene over undesirable CH_3OH overoxidation events. Accordingly, Cu-SSZ-13 was synthesized using the protocols demonstrated by Dinh et al. to maximize CH_3OH selectivity (i.e., using Si/Al <20, Cu contents of <0.3 Cu/cage, and synthesis gels void of Na ions) by avoiding the formation of undesirable Cu oxides that promote CH_3OH overoxidation.[11] H-ZSM-5 (Si/Al ≈ 15−19) was synthesized using protocols to prevent the incorporation of common Fe contaminants (<1 ppm as confirmed by inductively coupled plasma with optical emission spectroscopy (ICP-OES)). Cu-SSZ-13 and H-ZSM-5 powders were intimately mixed via vortexing prior to pelletizing in a 1:3 ratio by weight to reduce the length of CH_3OH diffusion paths to alkylation sites. Catalyst synthesis, composition, and characterization details are provided in the Experimental Methods section and Supporting Information Section 1A, Figures S1 and S2, and Table S1.

Scheme 1. Depiction of Product Protection Using a Copper-Exchanged Zeolite and a Second Proton-Form Zeolite of a Different Topology[a]

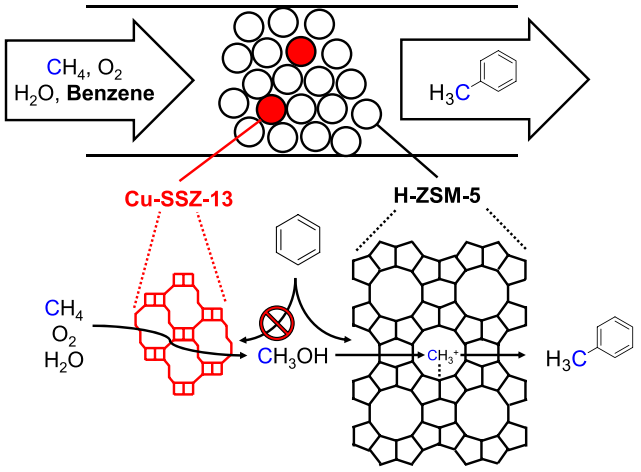

[a]The copper-exchanged zeolite produces an activated C_1 intermediate or CH_3OH that is incorporated into an aromatic cofeed over the Brønsted acid sites of the second zeolite.

As shown in Figure 1A,B (top), the Cu-SSZ-13/H-ZSM-5 mixture consistently generated increased rates of desirable products (i.e., CH_3OH, dimethyl ether (DME), or toluene) and lower rates of undesirable products (CO_2 and CO) compared to either Cu-SSZ-13 or H-ZSM-5 alone or the addition of the product formation rates over these individual beds (Figure S3). To compare the performance of individual

https://doi.org/10.1021/acscatal.1c02187
ACS Catal. 2021, 11, 9262−9270

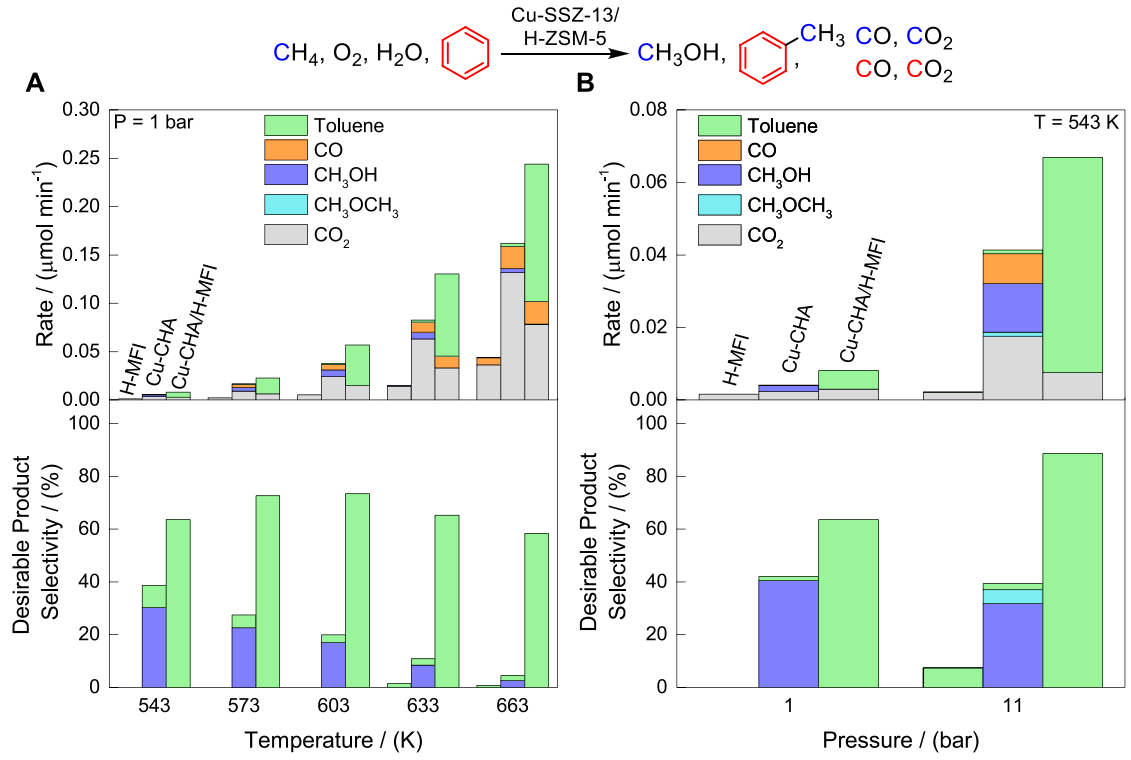

Figure 1. Total rates of product formation (top) and product selectivities (bottom) across (A) temperature and (B) pressure and over different catalyst compositions with the alkylation feed mixture: 0.2625 g H-ZSM-5-1, 0.0875 g Cu-SSZ-13-1, and (0.0875 g Cu-SSZ-13-1 + 0.2625 g H-ZSM-5-2), 26.1 sccm, y_{CH_4} = 0.18, $y_{C_6H_6}$ = 0.008, y_{O_2} = 0.001, P_{H_2O} = 3.1 kPa, bal He where y indicates mole fraction. Selectivities were estimated assuming all products were from CH_4. Estimated CH_4 conversions are provided in Table S3 and ranged from 0.003 to 0.08% over Cu-SSZ-13-1 and 0.004 to 0.13% over Cu-SSZ-13-1/H-ZSM-5-2. When pressurizing, water partial pressure remains unchanged because it was introduced by a saturator, all other reactants increased proportionally (Supporting Information Experimental Methods Section). The reaction schematic demonstrates potential sources of product formation where red and blue C's are indicative of the source of C (CH_4 or benzene) for the observed products.

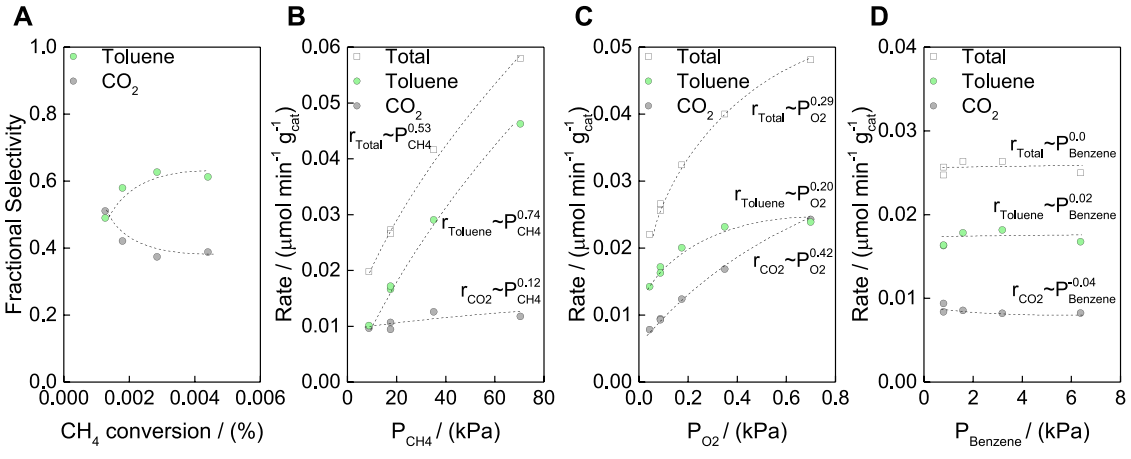

Figure 2. (A) Product selectivity versus conversion. Product formation rates versus (B) P_{CH_4}, (C) P_{O_2}, and (D) $P_{benzene}$ over (0.0875 g Cu-SSZ-13-1 + 0.2625 g H-ZSM-5-2), T = 543 K, P = 1 bar, 26.1 sccm, 3.2 kPa H_2O, 0.09 kPa O_2, 18 kPa CH_4, 0.80 kPa benzene, bal He, except as noted.

and mixed catalyst beds, product formation rates are reported in units of μmol/min and were observed under identical partial pressures, flow rates, and loadings of individual catalyst components across all experiments. Reaction rates were measured in the absence of heat and mass transfer limitations (Figure S4 and Table S2), with stable and repeatable product formation rates observed for at least 12 h on stream (Figure S5). Because CH_4 was fed in high molar excess and at low conversion, selectivity for a given product was defined as the product's rate of formation divided by the carbon-weighted sum of rates for all observed products. No additional products to those identified with gas chromatography coupled with mass spectroscopy (GC−MS) were detected. Cofeeding benzene with a standard mixture of CH_4, O_2, and H_2O at 1 bar and 663 K over the Cu-SSZ-13/H-ZSM-5 mixture resulted in a toluene selectivity of 58%. In contrast, 4% selectivity for partial oxidation products was measured for Cu-SSZ-13 alone (Figure 1A, bottom).

https://doi.org/10.1021/acscatal.1c02187
ACS Catal. 2021, 11, 9262−9270

Similarly, at 543 K and 11 bar, a toluene selectivity of 89% was obtained over Cu-SSZ-13/H-ZSM-5 compared to the 40% selectivity for partially oxidized products over Cu-SSZ-13 (Figure 1B, bottom). In all cases, although the Cu-SSZ-13/H-ZSM-5 mixture consistently featured higher CH_4 conversion values (Table S3) than the individual catalyst beds, the mixed system consistently featured drastically higher selectivity values. These results demonstrate that the combination of partial CH_4 oxidation with a chemical scavenging system is a viable solution to improving CH_4 conversion while maintaining high product selectivity.

Significant toluene formation is only observed when both Cu-SSZ-13 and H-ZSM-5 are used, indicating both catalysts are required for alkylation to occur. Control experiments showed than neither CH_3OH nor toluene was produced in the absence of a catalyst (Figure S6). We hypothesize the low toluene formation rates observed over Cu-SSZ-13 alone (Figure 1A,B) are a result of alkylation reactions catalyzed by acid sites on the surface of Cu-SSZ-13, while the low toluene formation rates over H-ZSM-5 at $T \geq 633$ K or $P > 1$ bar stem from the direct methylation formation of benzene with CH_4 over H-ZSM-5 as reported by Adebajo and coworkers.[20]

Kinetic experiments obtained by varying the total flow and partial pressures of CH_4, O_2, and benzene fed to Cu-SSZ-13/H-ZSM-5 (Figure 2) were used to map the different reaction pathways involved in a tandem partial oxidation and chemical scavenging system. The selectivity versus conversion plot shown in Figure 2A demonstrates that product formation proceeds by a combination of sequential and parallel reaction pathways. The presence of a sequential pathway is consistent with CH_4 activation first proceeding to CH_3OH and then to toluene and CO_2, in line with previous reports for CH_4 activation over Cu-SSZ-13.[11] The parallel reaction pathway can be attributed to the parallel formation of CO_2 from benzene alongside the formation of CO_2 and toluene from CH_3OH. The positive order dependence of the toluene formation rate upon CH_4 pressure implies that C−H scission is rate determining in the methylation reaction sequence (Figure 2B). This finding is consistent with the near first-order P_{CH_4} dependence previously reported for CH_4-to-CH_3OH formation over Cu-SSZ-13.[11] The weak order dependence for the rates of product formation on P_{O_2} are consistent with the dependences observed under CH_3OH synthesis conditions over Cu-SSZ-13 (Figure 2C).[11] The lack of observed gaseous CH_3OH in conjunction with zero-order dependence of all product formation rates upon benzene partial pressure implies rapid CH_3OH interception and sequential alkylation reactions. (Figure 2D). The proposed reaction pathway in Scheme 2 summarizes these observations where initial CH_4 activation forms CH_3OH which can either alkylate benzene to form toluene or undergo oxidation to CO_2. In parallel, benzene may also oxidize into CO_2 over Cu sites located on the surface of Cu-SSZ-13 or the H^+ sites of H-ZSM-5.

A separate set of experiments was conducted to investigate the effects of proximity and mixing of Cu-SSZ-13 and H-ZSM-5 upon rates of product formation and product selectivity (Figure 3). The rates of production formation over separate beds in series are compared to intimately mixed Cu-SSZ-13 and H-ZSM-5 and to the simple addition of product formation rates from individual beds of Cu-SSZ-13 and H-ZSM-5. Across a range of temperatures and pressures, two effects stand out as

Scheme 2. Hypothesized Reaction Pathway at Work in the Reported CH_4 Partial Oxidation/Aromatic Alkylation Mixed System[a]

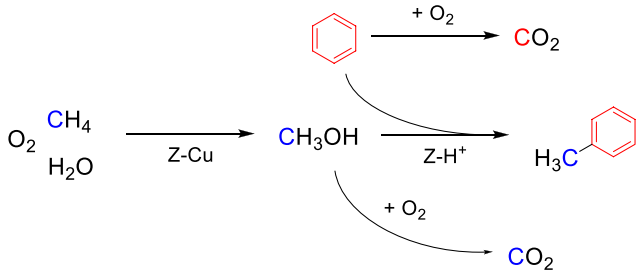

[a]Deleterious CO_2 formation from CH_3OH oxidation is minimized by intermediate scavenging to form alkylated aromatics, thus decreasing CO_2 yields, and direct benzene oxidation pathways can be mitigated by modification of catalyst morphology and gas phase compositions. CO is hypothesized to form by the same reaction pathways as CO_2 and is omitted for clarity.

the two catalyst beds are brought into closer contact: (1) the rate of toluene formation increases and (2) the rates of CO_2 and CO formation decrease. Consequently, intimately mixed Cu-SSZ-13 and H-ZSM-5 yielded the highest toluene selectivity of all catalyst configurations under identical conditions. These observations can be rationalized by the increased distance CH_3OH must be transported to be brought into contact with H-ZSM-5 with the separated beds, thereby increasing the number of homogeneous overoxidation events of CH_3OH and reducing the amount of CH_3OH available for benzene alkylation.

The desirable product selectivities reported in Figure 1A,B represent lower bounds because any CO_x generated from aromatic carbon combustion would decrease the observed selectivity compared to the true partial oxidation selectivity of CH_4-derived carbon. To identify and quantify the origin of undesirable products coming either from CH_4 or benzene oxidation, rates of product formation were measured over the same catalyst beds in the absence of benzene and CH_4, respectively, at 1 bar and temperatures ranging from 543 to 663 K. Figure 4A shows that, in the absence of benzene (i.e., feeding only $CH_4/H_2O/O_2$), CH_4 activation occurs primarily over Cu-SSZ-13. Across all temperatures, the total rate of C−H activation is similar between Cu-SSZ-13 and Cu-SSZ-13/H-ZSM-5, whereas the rate of C−H activation over H-ZSM-5 is negligible in comparison—a necessary requirement for the catalyst responsible for chemical scavenging. We speculate the absence of significant CH_3OH formation over Cu-SSZ-13/H-ZSM-5 can be attributed to the overoxidation of CH_3OH to CO_2 on additional nonselective sites within H-ZSM-5. Figure 4B demonstrates that benzene oxidation contributes substantially to the rates of CO and CO_2 formation in the absence of CH_4 (i.e., feeding only $C_6H_6/H_2O/O_2$). Although these results suggest that the contribution of benzene oxidation to CO and CO_2 product formation rates must be considered under tandem oxidation and alkylation conditions, the data cannot quantify the extent to which Cu-SSZ-13 and H-ZSM-5 each contribute to the observed product formation rates in the mixed system because the sum of the rates over the individual catalyst beds of H-ZSM-5 and Cu-SSZ-13 is not equal to the rates over Cu-SSZ-13/H-ZSM-5. To address this limitation, we performed an isotope switching experiment with $^{13}C_6H_6$ under

https://doi.org/10.1021/acscatal.1c02187
ACS Catal. 2021, 11, 9262−9270

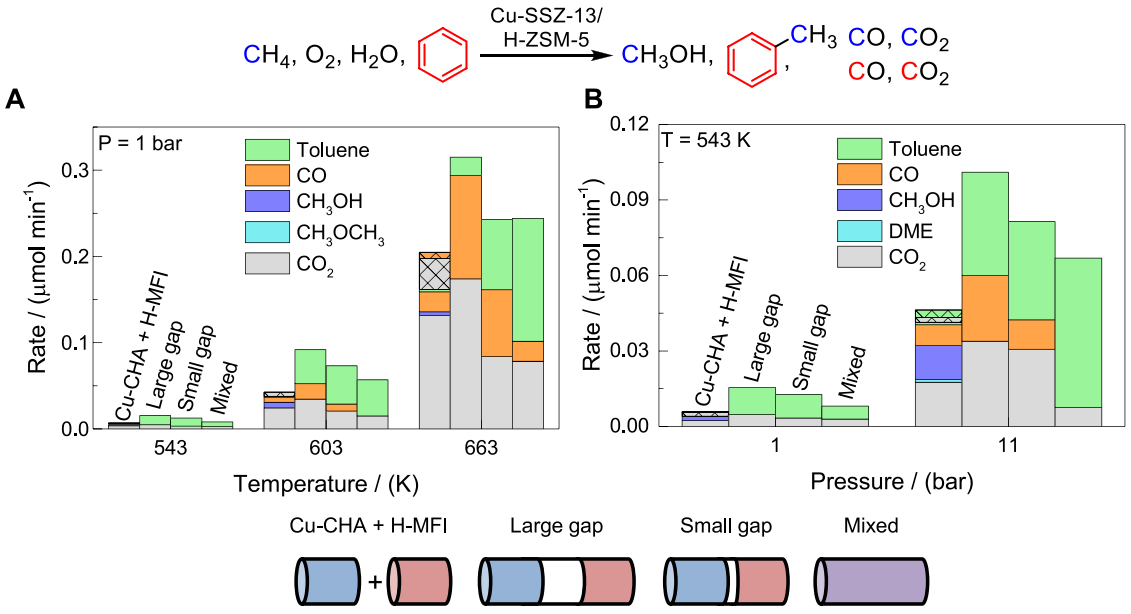

Figure 3. Comparison of the total rates of product formation across (A) temperature and (B) pressure over catalyst configurations with tandem oxidation and alkylation feed mixture. "Cu-SSZ-13 + H-ZSM-5" corresponds to the addition of rates of individual beds of Cu-SSZ-13 and H-ZSM-5 where these catalysts were tested separately in separate reactors, "Large gap" corresponds to a 3 cm quartz wool plug between beds, and "Small gap" corresponds to a 1 cm quartz wool plug. Bars with a crosshatch are rates observed over H-ZSM-5. "Mixed" corresponds to the mixture of 0.0875 g Cu-SSZ-13-1 and 0.2625 g H-ZSM-5-2. 26.1 sccm, y_{CH_4} = 0.18, $y_{C_6H_6}$ = 0.008, y_{O_2} = 0.001, P_{H_2O} = 3.1 kPa, bal He where y indicates mole fraction. When pressurizing, water partial pressure remains unchanged because it was introduced by a saturator, all other reactants increased proportionally. The reaction schematic demonstrates potential sources of product formation where red and blue C's are indicative of the source of C (CH_4 or benzene) for the observed products.

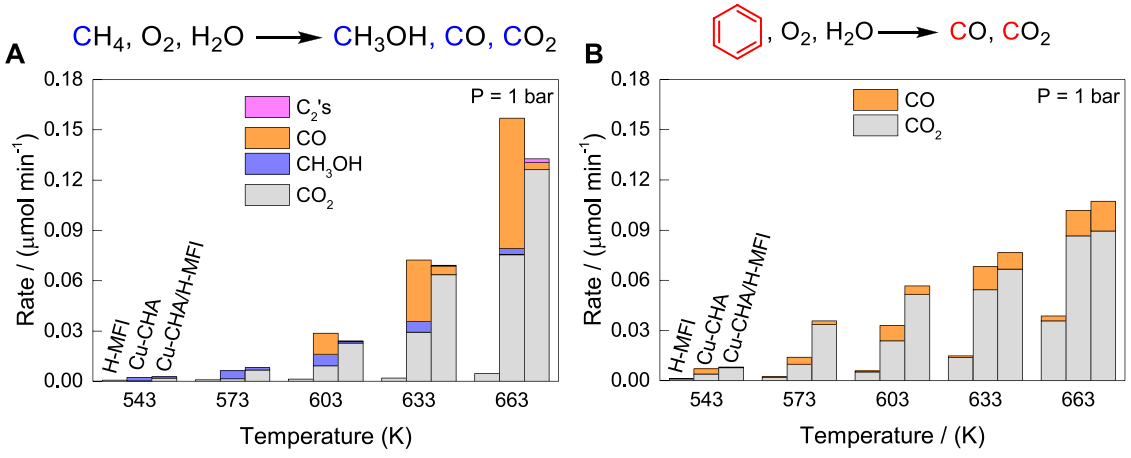

Figure 4. Comparison of the total rates of conversion and product formation under (A) partial CH_4 oxidation flows and (B) benzene oxidation flows over different catalyst compositions: 0.2625 g H-ZSM-5-1, 0.0875 g Cu-SSZ-13-1, and (0.0875 g Cu-SSZ-13-1 + 0.2625 g H-ZSM-5-1), P = 1 bar, 26.1 sccm, P_{CH_4} = 18 kPa, P_{O_2} = 0.09 kPa, P_{H_2O} = 3.1 kPa, $P_{C_6H_6}$ = 0.80 kPa, bal He. The reaction schematic demonstrates potential sources of product formation based where red and blue C's are indicative of the source of C (CH_4 or benzene) for the observed products.

tandem oxidation and alkylation conditions (cofeed of CH_4/O_2/H_2O/C_6H_6) over Cu-SSZ-13/H-ZSM-5 (Supporting Information Section 2A, Table S4, Figures S7 and S8). Benzene accounts for ca. 19% of the CO_2 observed at 543 K and 1 bar, and ca. 42% of the CO_2 at 603 K and 1 bar. Because benzene is fed in large excess compared to CO and CO_2 and its fragmentation pattern includes a fragment of m/z = 28, the contribution of benzene oxidation to CO formation was not estimated directly. These results were used to remove the contribution of benzene oxidation to CO_2 formation rates over Cu-SSZ-13/H-ZSM-5 and enable direct comparison of the rates of product formation from CH_4-to-CH_3OH over Cu-SSZ-13 to the rates of product formation from tandem oxidation and alkylation over Cu-SSZ-13/H-ZSM-5 (vide infra). Kinetic data in combination with these isotopic labeling experiments were used to estimate the contribution of benzene oxidation at conditions not specifically tested (Figure 2, Supporting Information Section 2B and Figure S9).

The results of the isotope labeling, bed proximity, and reaction kinetics experiments were used to correct for the contribution of benzene to CO_2 formation rates and enable the comparison between mixed and standalone beds. Figure 5A,B

https://doi.org/10.1021/acscatal.1c02187
ACS Catal. 2021, 11, 9262−9270

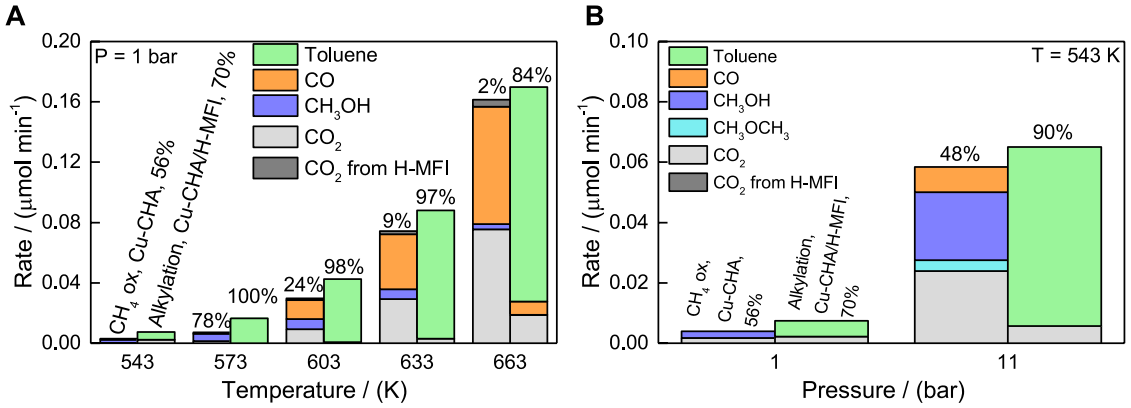

Figure 5. Comparison of rates of CH_4-to-CH_3OH over 0.0875 g Cu-SSZ-13-1 ("CH_4 Ox") to tandem partial oxidation and alkylation over (0.0875 g Cu-SSZ-13-1 + 0.2625 g H-ZSM-5-2) with removal of the contribution of benzene to CO_2 formation rates ("Alkylation") across (A) temperature and (B) pressure. Numbers above each bar are the carbon-weighted selectivities for partial oxidation products; 26.1 sccm, y_{CH_4} = 0.18, $y_{C_6H_6}$ = 0.008, y_{O_2} = 0.001, P_{H_2O} = 3.1 kPa, bal He where y indicates mole fraction. When pressurizing, water partial pressure remains unchanged because it was introduced by a saturator, all other reactants increased proportionally (Supporting Information Experimental Methods Section).

demonstrate that there is good agreement between the total rates of product formation over Cu-SSZ-13 for the conversion of CH_4-to-CH_3OH and for the conversion of CH_4-to-CH_3OH-to-toluene over Cu-SSZ-13/H-ZSM-5. Both catalyst beds contained the same loading of Cu-SSZ-13 but the bed used for tandem partial oxidation and alkylation contained additional H-ZSM-5. These results are consistent with CH_4 activation occurring primarily over Cu-SSZ-13 as previously discussed and enable facile observation of the improvement in desirable product selectivity under tandem partial oxidation and alkylation conditions. The slight differences in the total rate of C−H activation may be a result of (i) slight variations in Cu content between catalyst beds and/or (ii) the inability to precisely deconvolute the rates of CO formation from CH_4 and benzene. The improvement in partial oxidation selectivity is highlighted at 663 K and 1 bar where there is 77% selectivity for toluene over Cu-SSZ-13/H-ZSM-5 in contrast to 2% selectivity for CH_3OH over Cu-SSZ-13. The high selectivity for toluene at increasing conversion is indicative of the relatively fast scavenging of CH_3OH by toluene versus thermodynamically favorable deleterious overoxidation of free gaseous CH_3OH.

Increasing pressure for catalytic CH_4-to-CH_3OH conversion resulted in a small decrease in selectivity for CH_3OH (Figure 5B), in agreement with stoichiometric processes where selectivity is often minimally affected with pressure.[21,22] In contrast, positive orders previously reported for alkylation reactions over solid acids implicate higher rates at elevated pressures.[13] Indeed, increasing pressure under tandem oxidation and alkylation conditions over Cu-SSZ-13/H-ZSM-5 improved selectivity from 70 to 89%. This result can be explained by the total rate order dependence on reactant partial pressures for each product (e.g., with $r_{product} \sim P_{CH_4}{}^{a} P_{O_2}{}^{b}$, the total order dependence is $a + b$). Because toluene has a total dependence of 0.94 versus 0.54 for CO_2, increasing pressure increases the rate of toluene formation 75% more than the rate of CO_2 formation. In contrast, the rate of CH_3OH formation has a total order dependence of 1.03 versus 1.14 for the rate of CO_2 formation under CH_4-to-CH_3OH conditions over Cu-SSZ-13, consequently slightly favoring CO_2 formation at elevated pressures. Thus, under tandem partial oxidation and alkylation conditions, system pressure provides another handle for optimizing process conditions for selective CH_4 oxidation.

When plotting partial oxidation selectivity versus conversion for a slew of experimental observations, we demonstrate that the selectivity-conversion limit of CH_4 can be circumvented by scavenging CH_3OH (Figure 6). All data in this work were

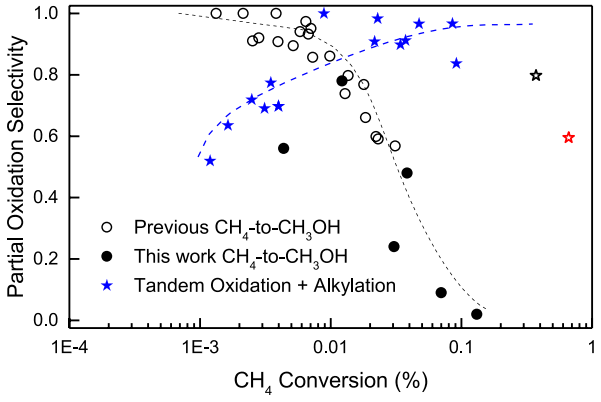

Figure 6. Selectivity for partially oxidized products versus conversion. "Open circles" were previously reported by Dinh et al.[11] "Black circles" were from this work and generated by varying temperature and pressure as in Figure 4A,B over 0.0875 g Cu-SSZ-13-1. Blue stars were generated by altering temperature, pressure, total flow rate, and catalyst loading over (0.0875 g Cu-SSZ-13-1 + 0.2625 g H-ZSM-5-2), and (0.366 g Cu-SSZ-13-2 + 1.097 g H-ZSM-5-3). The black and red open stars were generated in the same manner as the blue stars and also by increasing P_{O_2} by 3× and 5×, respectively. All conditions are summarized in Table S5. Baseline flow conditions: 26.1 sccm, y_{CH_4} = 0.18, $y_{C_6H_6}$ = 0.008, y_{O_2} = 0.001, P_{H_2O} = 3.1 kPa, bal He where y indicates mole fraction. When pressurizing, water partial pressure remains unchanged because it was introduced by a saturator, all other reactants increased proportionally.

generated by altering contact time, temperature, pressure, and catalyst loading and are summarized in Table S5, while product formation rates with increased catalyst loading are presented in Figure S10. To obtain increased catalyst loadings, a second batch of Cu-SSZ-13 was prepared. Comparable product formation rates to Cu-SSZ-13-1 were observed with the

https://doi.org/10.1021/acscatal.1c02187
ACS Catal. 2021, 11, 9262−9270

second batch (Figure S10). While Cu-SSZ-13 can produce CH_3OH with a selectivity >95% at low conversions, at the limit of 0.01% CH_4 conversion, the selectivity already decreases to <70%. In contrast, for the tandem system, a toluene selectivity >85% is maintained up to a CH_4 conversion of 0.1%. We note that the low toluene selectivity values observed below 0.01% CH_4 conversion may be a result of underestimation of the contribution of benzene oxidation at these conversions and competition between overoxidation of CH_3OH to CO_2 versus its diffusion to Brønsted acid sites. For the points at 0.4 and 0.7% CH_4 conversion, we increased P_{O_2} by 3× and 5×, respectively, to prevent oxygen starvation, resulting in slightly lower CH_3OH selectivities (see black and red stars in Figure 6) since oxygen concentrations were not optimized. Implementation of a tandem partial oxidation and alkylation system enabled us to surpass previously reported results for selectivity versus CH_4 conversion at mild conditions[11] while only requiring readily available O_2 and H_2O for CH_4 activation.

These results necessarily warrant comparison to the best performing stoichiometric processes for CH_4-to-CH_3OH conversion over Cu-exchanged zeolites and to other heterogeneous CH_4-to-CH_3OH systems. Sushkevich et al.[22] recently reported the optimization of an isothermal stoichiometric process over a Cu-FAU zeolite (Si/Al = 2.6, Cu/Al = 0.41, Cu wt% = 9.32) where the catalyst is first activated for 1 h under O_2 and then exposed to CH_4 for 1 h. Next, CH_3OH is desorbed for 1 h at 633 K with water vapor. Taking this process as a 3 h cycle time, the optimized CH_3OH yield was 2 μmol_{CH_3OH} min^{-1} g_{cat}^{-1} (93% selectivity). In comparison, we obtain a tandem oxidation and alkylation product yield of 1.7 $\mu mol_{Toluene}$ min^{-1} $g_{Cu\text{-}SSZ\text{-}13}^{-1}$ at 603 K and 11 bar (80% selectivity for toluene and xylene combined). When normalized on a Cu basis, our process translates to a rate of 12 $mmol_{CH_3OH}$ mol_{Cu}^{-1} min^{-1} compared to 1.4 $mmol_{CH_3OH}$ mol_{Cu}^{-1} min^{-1} reported for the optimized stoichiometric process. We surmise that the rates for the tandem system can be further increased by optimizing pressure, temperature, reactant partial pressures, and Cu loading in a similar fashion as was completed by Sushkevich et al. for the stochiometric process.[22]

This conversion and yield for tandem oxidation and alkylation are also comparable to the best performing heterogeneous catalysts for CH_4-to-CH_3OH conversion. Greater than 75% CH_3OH selectivity has been reported for heterogeneous catalysts at <2% CH_4 conversion.[8] However, with the exception of Cu-exchanged zeolites, the remaining heterogeneous catalysts require expensive oxidants such as H_2O_2[23] or N_2O[24] or extreme conditions (e.g., P > 140 bar).[25] Our system simply requires O_2, H_2O, and benzene as additional reactants and H-ZSM-5 as an additional catalyst at relatively mild conditions in comparison to these processes.

CONCLUSIONS

We have demonstrated the viability of product protection for CH_4 activation by first activating CH_4 over Cu-exchanged zeolites to produce CH_3OH and then capturing CH_3OH by aromatic alkylation over a proton-form zeolite. Control reactions and isotopically labeled benzene experiments demonstrate that benzene oxidation occurs in parallel to CH_4 activation and contributes to the observed CO and CO_2 formation rates. Upon accounting for benzene oxidation, the rates of CH_4 activation are comparable between Cu-SSZ-13 and Cu-SSZ-13/H-ZSM-5 across all conditions but selectivity for desirable products is markedly improved by chemically scavenging CH_3OH. High selectivity toward desirable products is maintained even above 0.1% CH_4 conversion where selectivity for CH_4-to-CH_3OH processes deteriorates. We report a toluene and xylene yield of 1.7 $\mu mol_{Toluene}$ min^{-1} $g_{Cu\text{-}SSZ\text{-}13}^{-1}$ at 603 K and 11 bar, greater than an optimized stoichiometric CH_4-to-CH_3OH system. Product protection, especially by chemical scavenging or by controlling molecular traffic of products and reagents,[26] is an important area of research to enable CH_4 activation, especially in the area of process optimization and catalyst design.

ASSOCIATED CONTENT

Supporting Information

The Supporting Information is available free of charge at https://pubs.acs.org/doi/10.1021/acscatal.1c02187.

Additional catalyst characterization details, $^{13}C_6H_6$ isotope switching experiment, estimation of benzene oxidation across conditions, and supporting figures referenced in the main text (PDF)

AUTHOR INFORMATION

Corresponding Author

Yuriy Román-Leshkov − *Department of Chemical Engineering, Massachusetts Institute of Technology, Cambridge, Massachusetts 02139, United States;* orcid.org/0000-0002-0025-4233; Email: yroman@mit.edu

Authors

Kimberly T. Dinh − *Department of Chemical Engineering, Massachusetts Institute of Technology, Cambridge, Massachusetts 02139, United States;* Present Address: Dow, Midland, Michigan 48674, United States; orcid.org/0000-0003-0657-1771

Mark M. Sullivan − *Department of Chemical Engineering, Massachusetts Institute of Technology, Cambridge, Massachusetts 02139, United States;* Present Address: Dow, Midland, Michigan 48674, United States; orcid.org/0000-0002-1765-4129

Pedro Serna − *ExxonMobil Research and Engineering, Annandale, New Jersey 08801, United States*

Randall J. Meyer − *ExxonMobil Research and Engineering, Annandale, New Jersey 08801, United States;* orcid.org/0000-0002-0679-0029

Complete contact information is available at: https://pubs.acs.org/10.1021/acscatal.1c02187

Notes

The authors declare no competing financial interest.

ACKNOWLEDGMENTS

The authors gratefully acknowledge the financial support of ExxonMobil. K.D. acknowledges the partial support from the National Science Foundation Graduate Research Fellowship under Grant No. 1122374. Any opinion, findings, and conclusions or recommendations expressed in this material are those of the author(s) and do not necessarily reflect the views of the National Science Foundation. This work made use of the MRSEC Shared Experimental Facilities at MIT, supported by the National Science Foundation under award

number DMR-14-19807. The authors thank Z. Wang for help with ICP-MS data collection and scientific discussion and S. Kwon for help with SEM and PXRD data collection.

REFERENCES

(1) Kondratenko, E. V.; Peppel, T.; Seeburg, D.; Kondratenko, V. A.; Kalevaru, N.; Martin, A.; Wohlrab, S. Methane conversion into different hydrocarbons or oxygenates: current status and future perspectives in catalyst development and reactor operation. *Catal. Sci. Technol.* **2017**, *7*, 366−381.

(2) Ahlquist, M.; Nielsen, R. J.; Periana, R. A.; Goddard Iii, W. A. Product Protection, the Key to Developing High Performance Methane Selective Oxidation Catalysts. *J. Am. Chem. Soc.* **2009**, *131*, 17110−17115.

(3) Shilov, A. E.; Shul'pin, G. B. Activation of C−H Bonds by Metal Complexes. *Chem. Rev.* **1997**, *97*, 2879−2932.

(4) Latimer, A. A.; Kakekhani, A.; Kulkarni, A. R.; Nørskov, J. K. Direct Methane to Methanol: The Selectivity−Conversion Limit and Design Strategies. *ACS Catal.* **2018**, *8*, 6894−6907.

(5) Colby, J.; Stirling, D. I.; Dalton, H. The soluble methane mono-oxygenase of Methylococcus capsulatus (Bath). Its ability to oxygenate n-alkanes, n-alkenes, ethers, and alicyclic, aromatic and heterocyclic compounds. *Biochem. J.* **1977**, *165*, 395−402.

(6) Periana, R. A.; Taube, D. J.; Gamble, S.; Taube, H.; Satoh, T.; Fujii, H. Platinum Catalysts for the High-Yield Oxidation of Methane to a Methanol Derivative. *Science* **1998**, *280*, 560−564.

(7) Hunter, N. R.; Gesser, H. D.; Morton, L. A.; Yarlagadda, P. S.; Fung, D. P. C. Methanol formation at high pressure by the catalyzed oxidation of natural gas and by the sensitized oxidation of methane. *Appl. Catal.* **1990**, *57*, 45−54.

(8) Ravi, M.; Ranocchiari, M.; van Bokhoven, J. A. The Direct Catalytic Oxidation of Methane to Methanol—A Critical Assessment. *Angew. Chem., Int. Ed.* **2017**, *56*, 16464−16483.

(9) Dinh, K. T.; Sullivan, M. M.; Serna, P.; Meyer, R. J.; Dincă, M.; Román-Leshkov, Y. Viewpoint on the Partial Oxidation of Methane to Methanol Using Cu- and Fe-Exchanged Zeolites. *ACS Catal.* **2018**, *8*, 8306−8313.

(10) Narsimhan, K.; Iyoki, K.; Dinh, K.; Román-Leshkov, Y. Catalytic Oxidation of Methane into Methanol over Copper-Exchanged Zeolites with Oxygen at Low Temperature. *ACS Cent. Sci.* **2016**, *2*, 424−429.

(11) Dinh, K. T.; Sullivan, M. M.; Narsimhan, K.; Serna, P.; Meyer, R. J.; Dincă, M.; Román-Leshkov, Y. Continuous Partial Oxidation of Methane to Methanol Catalyzed by Diffusion-Paired Copper Dimers in Copper-Exchanged Zeolites. *J. Am. Chem. Soc.* **2019**, *141*, 11641−11650.

(12) Yashima, T.; Ahmad, H.; Yamazaki, K.; Katsuta, M.; Hara, N. Alkylation on synthetic zeolites: I. Alkylation of toluene with methanol. *J. Catal.* **1970**, *16*, 273−280.

(13) Kaeding, W. W.; Chu, C.; Young, L. B.; Weinstein, B.; Butter, S. A. Selective alkylation of toluene with methanol to produce para-Xylene. *J. Catal.* **1981**, *67*, 159−174.

(14) Kennedy, E. M.; Lonyi, F.; Ballinger, T. H.; Rosynek, M. P.; Lunsford, J. H. Conversion of benzene to substituted aromatic products over zeolite catalysts at elevated pressures. *Energy Fuels* **1994**, *8*, 846−850.

(15) Baerlocher, C.; McCusker, L. B. *Database of Zeolite Structures*. International Zeolite Association, 2016.

(16) Baertsch, C. D.; Funke, H. H.; Falconer, J. L.; Noble, R. D. Permeation of Aromatic Hydrocarbon Vapors through Silicalite−Zeolite Membranes. *J. Phys. Chem.* **1996**, *100*, 7676−7679.

(17) Di Iorio, J. R.; Gounder, R. Controlling the Isolation and Pairing of Aluminum in Chabazite Zeolites Using Mixtures of Organic and Inorganic Structure-Directing Agents. *Chem. Mater.* **2016**, *28*, 2236−2247.

(18) Martínez-Franco, R.; Moliner, M.; Thogersen, J. R.; Corma, A. Efficient One-Pot Preparation of Cu-SSZ-13 Materials using Cooperative OSDAs for their Catalytic Application in the SCR of NOx. *ChemCatChem* **2013**, *5*, 3316−3323.

(19) Ren, L.; Zhu, L.; Yang, C.; Chen, Y.; Sun, Q.; Zhang, H.; Li, C.; Nawaz, F.; Meng, X.; Xiao, F.-S. Designed copper−amine complex as an efficient template for one-pot synthesis of Cu-SSZ-13 zeolite with excellent activity for selective catalytic reduction of NO_x by NH_3. *Chem. Commun.* **2011**, *47*, 9789−9791.

(20) Adebajo, M. O.; Howe, R. F.; Long, M. A. Methylation of Toluene with Methane over ZSM-5 Catalysts. *Energy Fuels* **2001**, *15*, 671−674.

(21) Tomkins, P.; Mansouri, A.; Bozbag, S. E.; Krumeich, F.; Park, M. B.; Alayon, E. M.; Ranocchiari, M.; van Bokhoven, J. A. Isothermal Cyclic Conversion of Methane into Methanol over Copper-Exchanged Zeolite at Low Temperature. *Angew. Chem., Int. Ed.* **2016**, *55*, 5467−5471.

(22) Sushkevich, V. L.; van Bokhoven, J. A. Methane-to-Methanol: Activity Descriptors in Copper-Exchanged Zeolites for the Rational Design of Materials. *ACS Catal.* **2019**, *9*, 6293−6304.

(23) Hammond, C.; Forde, M. M.; Ab Rahim, M. H.; Thetford, A.; He, Q.; Jenkins, R. L.; Dimitratos, N.; Lopez-Sanchez, J. A.; Dummer, N. F.; Murphy, D. M.; Carley, A. F.; Taylor, S. H.; Willock, D. J.; Stangland, E. E.; Kang, J.; Hagen, H.; Kiely, C. J.; Hutchings, G. J. Direct Catalytic Conversion of Methane to Methanol in an Aqueous Medium by using Copper-Promoted Fe-ZSM-5. *Angew. Chem., Int. Ed.* **2012**, *51*, 5129−5133.

(24) Panov, G. I.; Sobolev, V. I.; Dubkov, K. A.; Parmon, V. N.; Ovanesyan, N. S.; Shilov, A. E.; Shteinman, A. A. Iron complexes in zeolites as a new model of methane monooxygenase. *React. Kinet. Catal. Lett.* **1997**, *61*, 251−258.

(25) Boomer, E. H.; Thomas, V. The Oxidation of Methane at High Pressures: III. Experiments Using Pure Methane and Principally Copper as Catalyst. *Can. J. Res.* **1937**, *15b*, 414−433.

(26) Jin, Z.; Wang, L.; Zuidema, E.; Mondal, K.; Zhang, M.; Zhang, J.; Wang, C.; Meng, X.; Yang, H.; Mesters, C.; Xiao, F.-S. Hydrophobic zeolite modification for in situ peroxide formation in methane oxidation to methanol. *Science* **2020**, *367*, 193.

https://doi.org/10.1021/acscatal.1c02187
ACS Catal. 2021, 11, 9262−9270